Surface plasmon enhanced photoconductance and single electron effects in mesoporous titania nanofibers loaded with gold nanoparticles

Min-Soo Son,[1] Ji-Eun Im,[2] Kang-Kyun Wang,[2] Seung-Lim Oh,[2] Yong-Rok Kim,[2,a)] and Kyung-Hwa Yoo[3,b)]
[1]*Department of Physics, Yonsei University, 134 Sinchon-dong, Seodaemun-gu, Seoul 120-749, Republic of Korea*
[2]*Department of Chemistry, Yonsei University, 134 Sinchon-dong, Seodaemun-gu, Seoul 120-749, Republic of Korea*
[3]*Department of Physics and National Core Research Center for Nanomedical Technology, Yonsei University, 134 Sinchon-dong, Seodaemun-gu, Seoul 120-749, Republic of Korea*

(Received 31 August 2009; accepted 17 December 2009; published online 15 January 2010)

We have synthesized mesoporous TiO_2 nanofibers loaded with Au nanoparticles (MTNF-Au) and fabricated single nanofiber-based devices. MTNF-Au devices exhibited surface plasmon enhanced photoconductance under visible light, whereas MTNF devices without Au nanoparticles did not. Moreover, Coulomb oscillations were observed at 4.2 K in MTNF-Au devices, indicating that Au nanoparticles embedded in MTNF-Au played a role of Coulomb islands. These results suggested that the enhanced photoconductance was ascribed to electron tunneling of hot electrons generated by the surface plasmon resonance. © *2010 American Institute of Physics*. [doi:10.1063/1.3291052]

Metal-dielectric nanocomposites have received considerable attention because of their unusual electrical and optical properties.[1,2] Noble metal nanoparticles, such as Au and Ag, embedded in a dielectric matrix exhibit surface plasmon resonance (SPR) in the visible region due to the interaction of light with electrons at the metal-dielectric interface.[3–9] This SPR resonance wavelength strongly depends on the size and shape of nanoparticles, the interparticle distance, and the dielectric properties of the surrounding medium.[4–8] Thus, the metal-dielectric nanocomposites offer significant potential as materials showing enhanced or tunable harnessing of light.

Among various nanocomposites, titania (TiO_2)-based nanocomposites are of particular interest for applications for energy conversion. In photovoltaic and photoelectrochemical cells, TiO_2 has been widely used as a photoanode.[10] However, TiO_2 absorbs only UV light ($\lambda < 388$ nm) due to the large band gap of 3.0–3.2 eV, so that its conversion efficiency is low. A possible strategy to improve the efficiency of energy conversion is to enhance the efficiency of visible light absorption since the maximum amount of energy of the solar spectrum lies in the visible range from ~1.4 to 3.0 eV.[11] Therefore, a nanocomposite consisting of metal nanoparticles embedded in a TiO_2 matrix has emerged as an attractive material to enhance the energy conversion efficiency. In fact, Au–TiO_2 nanocomposite films have been synthesized and plasmon-induced photocurrents have been reported in an electrolyte under visible light.[9]

In an effort to obtain a material with improved absorption of visible light, we fabricated a Au–TiO_2 nanocomposite with a one-dimensional (1D) morphology by synthesizing mesoporous TiO_2 nanofibers (MTNF) which were then loaded with Au nanoparticles within the pores of the MTNF (MTNF-Au). As expected, the SPR absorption in the visible region was observed in MTNF-Au, but not in MTNF. For transport measurements, single nanofiber-based devices were fabricated and their plasmon-induced photocurrents were measured under visible light. In addition, we also carried out low temperature transport measurements to investigate the effects of Au nanoparticles on the electronic transport properties.

The MTNF was synthesized, as previously reported.[12] In brief, the porous alumina membranes (pore diameter: ~200 nm and thickness: ~60 μm) purchased from Whatman (Anodisc 13) were dipped into the lyotropic precursor solutions and stirred for 12 h to fill completely the porous alumina channels with the precursor solutions. The lyotropic precursor solution consisted of a triblock copolymer of Pluronic F127 (BASF Chemical Co., New Jersey, USA) and a titanium precursor in an acidic ethanol solution as follows: 1 g of Pluronic F127 was homogeneously mixed with 2.84 g of titanium(IV) isopropoxide (Acros Organics, 98+%, New Jersey, USA) and 1.86 g of hydrochloric acid (Matsunden Chemical Co., 35%, Osaka, Japan) in 2.3 g of ethanol (Merck KGaA; Catalogue No. 111727, 99.9>%, Darmstadt, Germany) for 2 h. The porous alumina membrane including the precursor solution was allowed to gelate at 60 °C for 48 h. The specimens were calcined at 500 °C in air for 6 h to eliminate the surfactant included in the MTNF and the porous alumina membrane was removed using a 5 M hydrochloric acid solution to obtain MTNFs. Subsequently, nanometer-sized Au particles were loaded within the pores of MTNF by the deposition-precipitation method using $HAuCl_4$ as a precursor material.[13,14] An aqueous solution of 4.86×10^{-3} M $HAuCl_4 \cdot 4H_2O$ (Kanto Chemicals, >99.9%) in 50 mL H_2O was heated to 70 °C and was adjusted to pH 7.0 by using 1 M NaOH (aqueous). Then, the prepared MTNFs were suspended in the solution by stirring and the solution was aged at 70 °C for 3 h. Finally, the nanofibers were washed several times with distilled water, dried under vacuum, and calcined at 923 K in ambient air for 4 h. Figure 1(a) shows a transmission electron microscope (TEM) image of the MTNF. The typical diameter and the length of the MTNFs were ~200 nm and 10 μm, respectively, with an average pore size of approximately 10 nm. Au nanoparticles

a)Electronic mail: yrkim@yonsei.ac.kr.
b)Electronic mail: khyoo@yonsei.ac.kr.

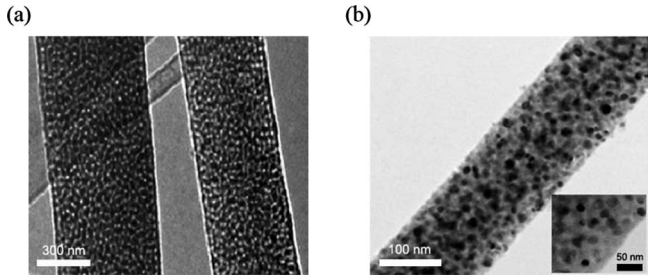

FIG. 1. TEM images of MTNF (a) and MTNF-Au (b).

were loaded within the pores of MTNF by the deposition-precipitation method [Fig. 1(b)]. Nearly all pores were filled with Au nanoparticles, whose diameters were similar to the MTNF pore size.

The UV-visible absorption spectra were measured using a V-550 diffuse reflectance spectrophotometer (JASCO) for MTNF and MTNF-Au deposited on quartz substrates [Fig. 2(a)]. Both MTNF and MTNF-Au exhibited large absorptions in the UV region due to the large energy band gap of TiO_2. However, in the visible range, MTNF-Au revealed a pronounced SPR absorption peak at ~570 nm, while MTNF exhibited almost no absorption.

For electronic transport measurements, single nanofiber-based devices were fabricated on a heavily doped Si substrate with a 200 nm thick thermally grown SiO_2 layer by electron-beam lithography and lift-off techniques, as shown in inset of Fig. 2(b). Source and drain electrical contacts to the nanofiber were made via evaporated Au/Cr (1000 nm/10 nm) electrodes and the heavily doped Si substrate was used as a gate electrode. The electrical measurements were carried out using a semiconductor characterization (Agilent 4155C). For both MTNF and MTNF-Au devices, the source/drain current (I)-voltage (V) curve was linear at room temperature and the typical room temperature resistance was estimated to

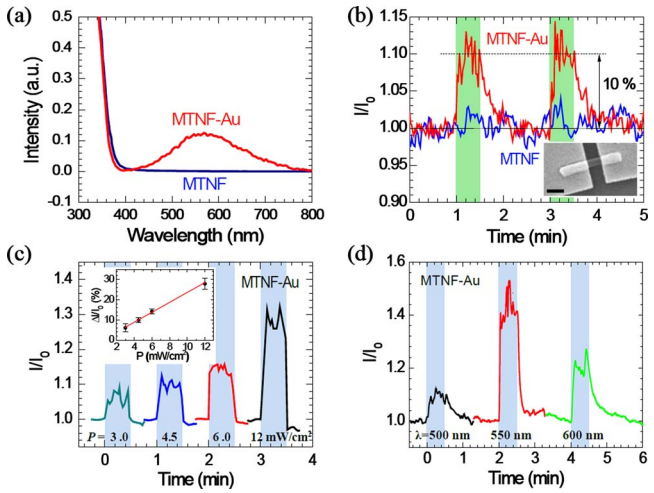

FIG. 2. (Color online) (a) UV-visible absorption of MTNF and MTNF-Au. (b) Photoresponse to the light of λ=500 nm with the power density of 6 mW/cm^2 for MTNF and MTNF-Au devices. The inset shows a SEM image of the fabricated single nanofiber-based device. Scale bar: 500 nm. (c) Photoresponse to the light of λ=510 nm with the power density of 3, 4.5, 6, and 12 mW/cm^2 for MTNF-Au device. The inset is the plot of the photocurrent vs the power density. (d) Photoresponse to the light of λ=500, 550, and 600 nm with the power density of 6 mW/cm^2 for the MTNF-Au device. Shaded and unshaded regions mark the light-on and light-off periods, respectively.

be 2–3 MΩ. To determine whether the absorbed light via SPR can contribute to increased conductance, the photoresponse to 500 nm light with power (P) of 6 mW/cm^2 was measured for the MTNF and MTNF-Au devices [Fig. 2(b)]. During irradiation with 500 nm light, the current of the MTNF-Au device increased about 10%, whereas the current of the MTNF device was barely changed, indicating that the enhanced photocurrents under 500 nm light could be ascribed to the SPR absorption. Figure 2(c) shows the photoresponse to 510 nm light with different power intensities (P=3, 4.5, 6, and 12 W/cm^2). A linear relationship was found between the photocurrent and the power density [the inset of Fig. 2(c)], suggesting that the effects of space charge were negligible.[15] In addition, we also investigated the dependence of the incident wavelength on the photocurrent. When the MTNF-Au device was irradiated with light of different wavelengths (λ=500, 550, and 600 nm; P =6 mW/cm^2), the photocurrent increased by about 10%, 40%, and 20%, respectively [Fig. 2(d)]. These wavelength-dependent photocurrents verified that the photocurrent in the visible range was induced by the SPR absorption.

Similar enhancement of the photoconductance has also been reported for Au nanoparticle-embedded-silica nanowires[3] and Au nanoparticle monolayers,[4,16] in which electron tunneling of hot electrons through the oxide barrier[3,4] or a bolometric effect[16] were proposed as possible conduction mechanisms of the plasmon-induced photocurrent. In our MTNF-Au device, the current slowly returned to the initial value after the light source was turned off [Figs. 2(b)–2(d)]. Thus, to clarify whether the plasmon-induced photocurrents observed in the MTNF-Au device were due to bolometric effects, we used an IR camera (Fluke-62) to measure the temperature of MTNF and MTNF-Au deposited on quartz substrates upon irradiation with 550 nm light at P =6 mW/cm^2. The temperature was almost identical for both MTNF and MTNF-Au, indicating that the plasmon-induced photocurrent observed in MTNF-Au was not attributable to photothermal effects. We, therefore, considered that the enhanced photoresponse behaviors in the MTNF-Au devices were possibly due to generation of hot electrons and electron tunneling through the Schottky barriers formed at the interface of the Au nanoparticles and the TiO_2 matrix.[17]

In addition to photoresponsive behaviors, we also measured the temperature-dependent I-V characteristics to investigate the effects of Au nanoparticles embedded in TiO_2 on the electronic transport properties. The I-V curves measured at several temperatures are shown in Figs. 3(a) and 3(b) for MTNF and MTNF-Au devices, respectively. For both devices, the I-V curves were linear at room temperature, but became nonlinear as the temperature decreased. In Fig. 3(c), the differential zero-bias conductance, $G=dI/dV$ at $V=0$ V, is plotted as a function of $1/T$ for MTNF and MTNF-Au devices. G of the MTNF device was well described by the Arrhenius relationship of $G \propto \exp(-E_a/k_BT)$ with an activation energy of $E_a \approx 0.1$ eV. Although $E_a=0.1$ eV was much smaller than the energy gap of TiO_2, presumably because of defect states, the observed temperature dependence might be ascribed to the semiconducting properties of TiO_2. On the other hand, the MTNF-Au device exhibited two different slopes depending on the temperature [Fig. 3(c)]. At T >200 K, we estimated a value of $E_a \approx 0.1$ eV in MTNF-Au device, whereas at $T<200$ K, we obtained $E_a \approx 0.03$ eV,

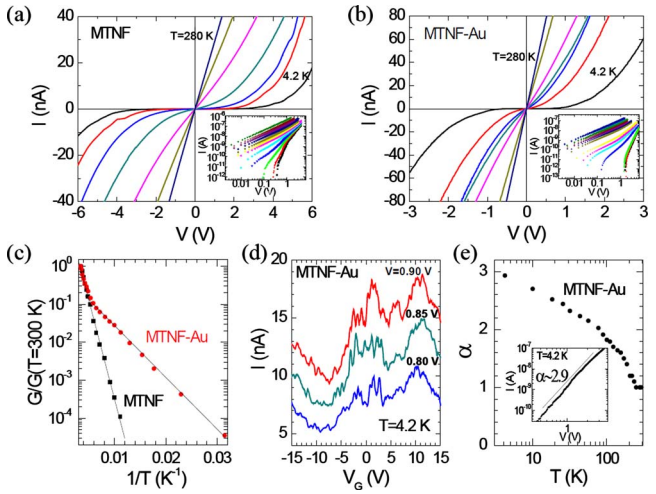

FIG. 3. (Color online) The *I-V* curves measured at various temperatures (4.2, 77, 110, 155, 205, 250, and 280 K) for MTNF (a) and MTNF-Au (b) devices. The insets show *I-V* curves in log-log scales. (c) The differential conductance G at zero-bias voltage as a function of $1/T$. (d) I-V_G plot measured at 4.2 K for the MTNF-Au device. (e) The values of α estimated from the data of the MTNF-Au device as a function of temperature. The inset is the *I-V* curve measured at 4.2 K for the MTNF-Au in log-log scales.

implying that the presence of Au nanoparticles in the MTNF-Au device influenced the electrical transport properties at low temperatures, but not at high temperatures. Au nanoparticles embedded in TiO_2 were electrically isolated from each other, and thus may be regarded as Coulomb islands. Moreover, since models of electron transport in an array of identical Coulomb islands predict a thermally activated behavior of the zero-bias conductance, $G \propto \exp(-E_a/k_B T)$,[18] $E_a \approx 0.03$ eV obtained for $T < 200$ K is probably explained by the energy required to charge an electrically neutral nanoparticle.

To confirm that Au nanoparticles embedded in TiO_2 act as Coulomb islands, we measured the source/drain current (I)-gate voltage (V_G) characteristics at $T=4.2$ K, where the highly doped Si was used as the bottom gate. Indeed, Coulomb oscillations with periodicity of $\Delta V_G \approx 11$ V were observed [Fig. 3(d)], although the small oscillations resulting from the capacitive coupling among Au nanoparticles were superimposed. For comparison, we also measured the I-V_G curves at 4.2 K for MTNF devices. In contrast to MTNF-Au devices, MTNF devices showed no oscillation, supporting that Au nanoparticles in MTNF-Au had a relatively uniform size distribution and could be considered as an array of Coulomb islands.

For a uniform array of metal islands, a theory[19] predicts the *I-V* characteristics to follow the relationship

$$I \propto (V/V_T - 1)^{\alpha}, \tag{1}$$

for $V/V_T > 1$, where V_T is a threshold voltage below which the current is zero and α is a scaling exponent reflecting the dimensionality of the accessible current-conducting pathways. According to the theoretical simulations for arrays of finite size, $\alpha = 1.0$ and 2.0 ± 0.2 were given for one and two dimensions,[19] respectively, and $\alpha \approx 2.7 \sim 3.0$ was experimentally found for the three-dimensional (3D) Au nanocrystal/silica arrays.[20] To estimate the scaling exponent α for our devices, the measured *I-V* curves were plotted in log-log scales [insets of Figs. 3(a) and 3(b)] and α was calculated from the slopes at high voltages. A plot of the estimated values of α as a function of T for the MTNF-Au device revealed that α increased with decreasing temperature [Fig. 3(e)]. The value of α at 4.2 K was calculated to be approximately 2.9, implying that the MTNF-Au nanostructure may be considered as a 3D assembly of Au nanoparticles.

In summary, we have synthesized MTNF loaded with Au nanoparticles (MTNF-Au) and fabricated single nanofiber-based devices on SiO_2/Si substrates. Upon illumination with visible light, the MTNF-Au device exhibited wavelength, power-dependent and reversible photoresponses, which were caused by the SPR absorption. In addition, we also investigated the temperature dependence of electronic transport properties for both the MTNF and MTNF-Au devices. These two devices differed in their temperature dependence at low temperatures. In particular, the single electron effects were demonstrated in the MTNF-Au device, suggesting that the variations in temperature difference were attributable to electronic tunneling among the Au nanoparticles embedded in the TiO_2.

This work has been financially supported by National Research Foundation of Korea through National Core Research Center for Nanomedical Technology (Grant No. R15-20040924-00000-0) and a grant from the Korea Healthcare technology R&D Project, Ministry for Health, Welfare & Family Affairs, Republic of Korea (Grant No. A085136). J.E.I., K.K.W., and S.L.O. acknowledge the fellowship of the BK 21 program from the Ministry of Education and Human Resources Development.

[1] T. Tanaka, IEEE Trans. Dielectr. Electr. Insul. **12**, 914 (2005).
[2] F. Hache, D. Ricard, and C. Flytzanis, J. Opt. Soc. Am. B **3**, 1647 (1986).
[3] M.-S. Hu, H.-L. Chen, C.-H. Shen, L.-S. Hong, B.-R. Huang, K.-H. Chen, and L.-C. Chen, Nature Mater. **5**, 102 (2006).
[4] J. Tang, H. Rong, X. Li, B. Zou, and J. Li, ChemPhysChem **8**, 1611 (2007).
[5] S. L. Link and M. A. El-Sayed, J. Phys. Chem. B **103**, 8410 (1999).
[6] R. Jin, Y. W. Cao, C. A. Mirkin, K. L. Kelly, G. C. Schatz, and J. G. Zheng, Science **294**, 1901 (2001).
[7] J. J. Mock, M. Barbic, D. R. Smith, D. A. Schultz, and S. Schultz, J. Chem. Phys. **116**, 6755 (2002).
[8] K. Matsubara and T. Tatsuma, Adv. Mater. **19**, 2802 (2007).
[9] Y. Tian and T. Tatsuma, J. Am. Chem. Soc. **127**, 7632 (2005).
[10] M. Grätzel, Nature (London) **414**, 338 (2001).
[11] T. Bak, J. Nowotny, M. Rekas, and C. C. Sorrel, Int. J. Hydrogen Energy **27**, 991 (2002).
[12] W.-S. Chae, S.-W. Lee, and Y.-R. Kim, Chem. Mater. **17**, 3072 (2005).
[13] S. H. Overbury, L. Ortiz-Soto, H. Zhu, B. Lee, M. D. Amiridis, and S. Dai, Catal. Lett. **95**, 99 (2004).
[14] H. Tada, T. Soejima, S. Ito, and H. Kobayashi, J. Am. Chem. Soc. **126**, 15952 (2004).
[15] A. M. Goodman and A. Rose, J. Appl. Phys. **42**, 2823 (1971).
[16] M. A. Mangold, C. Weiss, M. Calame, and A. W. Holleitner, Appl. Phys. Lett. **94**, 161104 (2009).
[17] M. Jakob, H. Levanon, and P. V. Kamat, Nano Lett. **3**, 353 (2003).
[18] C. A. Neugebauer and M. B. Webb, J. Appl. Phys. **33**, 74 (1962).
[19] A. A. Middleton and N. S. Wingreen, Phys. Rev. Lett. **71**, 3198 (1993).
[20] H. Fan, K. Yang, D. M. Boye, T. Sigmon, K. J. Malloy, H. Xu, G. P. López, and C. J. Brinker, Science **304**, 567 (2004).